# DESIGN CONSIDERATIONS FOR ASTRONOMICAL ECHELLE SPECTROGRAPHS

DANIEL J. SCHROEDER*
Department of Physics
Beloit College

*Received July 23, 1970*

Principles common to the design of all spectrographs using echelles as the main dispersing element and gratings for the cross dispersion are discussed. Consideration is given to the possibilities of a Cassegrain echelle spectrograph for an *f*/8 beam, and a comparison of its features with those of conventional grating spectrographs. Results are presented in a form which makes them useful for echelle spectrograph design for any telescope.

## Introduction

The development of high-quality replica echelle gratings within the past few years has aroused great interest on the part of many astronomers and has led to an increased use of echelles for stellar astronomy. To date, descriptions of echelle spectrographs used primarily for stellar astronomy, and results obtained with them, have been reported by Kopylov and Steshenko (1965), Liller (1970), and Schroeder and Anderson (1970). There are several advantages of an instrument with an echelle as the principal dispersing element, when compared with a conventional grating instrument.

1. Because of the higher angular dispersion of an echelle, it is feasible to build a spectrograph which fits easily at the Cassegrain focus of a medium-sized telescope, but for which the plate factors are like those normally obtained only by large coudé spectrographs. The advantage is that more light is available at the spectrograph entrance slit because the extra mirrors required to reach the coudé focus are eliminated. For the University of Wisconsin Cassegrain echelle instrument (Schroeder and Anderson 1970), a plate factor of 1.9 Å/mm at λ 5000 is achieved with a camera focal length of 75 cm.

---

*Visiting Astronomer, Kitt Peak National Observatory, which is operated by the Association of Universities for Research in Astronomy, Inc., under contract with the National Science Foundation.

2. For a given collimator diameter and entrance-slit angular width, as projected on the sky, an echelle instrument will have better spectral resolution. An alternative statement is that for a given spectral resolution an echelle spectrograph has larger throughput than a grating instrument. The advantage of the echelle can easily be a factor of three or more.

3. The separation of various echelle orders requires a crossed dispersing element which gives a two-dimensional output format particularly suited to image tubes. Though the introduction of this extra dispersing element means a decreased overall efficiency, the advantage of recording large amounts of spectral data on a single image-tube exposure is significant. For example, at reciprocal dispersions of 2 Å/mm–3 Å/mm, an image-tube photocathode 40 mm in diameter will accept 2000 Å–3000 Å of spectrum from an echelle instrument, as compared with approximately 100 Å of spectrum such a tube will accept from a comparable coudé spectrograph. The background for each of these advantages is developed in detail below.

A study of possible Cassegrain echelle spectrograph designs was prompted by development of instrumentation for the 4.0-meter telescopes, *f*/7.8 Cassegrain, now being built by Kitt Peak National Observatory and Cerro Tololo Inter-American Observatory. The echelle spectrographs built so far are used in considerably slower beams. The intent of this paper is to describe the properties of echelle spectrographs, in a general way, so that anyone considering such an instrument can quickly see what it is capable of on any given telescope. As an example, an optical layout is shown for an *f*/7.8 beam, though it is adaptable to any focal ratio. Reasons for the optical arrangement selected are given. In addition to the general features of echelle instruments, a comparison of these features with those of conventional high-dispersion grating spectrographs is also given, so that the advantages of echelles are more easily seen.

## Echelle Properties

The general theory of the echelle has been discussed by Harrison (1949) and Schroeder (1967) for the case where the angles of incidence and diffraction on the echelle are equal. Because in practice

the diffracted beam must be separated from the incident beam, the treatment here will take this requirement into account. The angular separation of the incident and diffracted beams has a significant effect on the angular dispersion; this effect is considered below.

An echelle is a rather coarse diffraction grating (30-300 grooves/mm) used at a large angle of incidence (blaze angle typically 63°.5) in a high order of interference (typically 10–100). The echelle is shown in Figure 1, in which an arbitrary ray strikes the echelle at O,

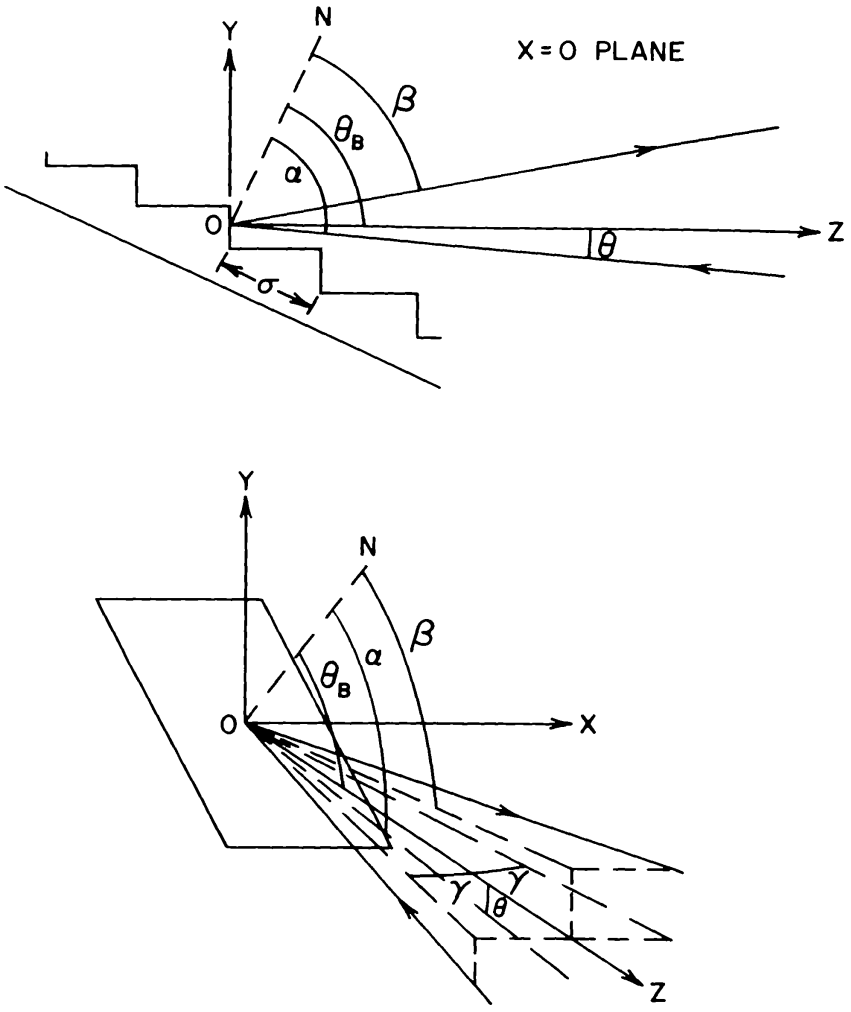


FIG. 1 — Local coordinate system for an arbitrary ray striking the echelle at O, where the $z$ axis is perpendicular to an echelle facet, and ON denotes the echelle normal. See text following equation (1) for definitions of symbols.

the origin of the local coordinate system for that ray. The $x$-axis is along an echelle groove; the $y = 0$ plane makes angle $\theta_B$ with the echelle normal where $\theta_B$ = blaze angle. The diffraction equation of the echelle is

$$m\lambda/\sigma = \cos\gamma\,(\sin\alpha + \sin\beta) \quad , \tag{1}$$

where $m$ is the order number for wavelength $\lambda$, $\sigma$ is the grating constant, $\alpha$ and $\beta$ are the angles of incidence and diffraction, respectively, measured in the $yz$-plane, and $\gamma$ is the angle between the incident ray and the $yz$-plane. The factor of $\cos\gamma$ is a consequence of the apparent foreshortening of the groove spacing when $\gamma \neq 0$, a situation which can occur when the light from a collimator is dispersed by a cross-dispersion element before reaching the echelle. From Figure 1 we see that $\alpha = \theta_B + \theta$ and, at the peak of the blaze, $\beta = \theta_B - \theta$. Hence at the blaze peak we have $m\lambda/\sigma = 2\cos\gamma\cos\theta\sin\theta_B$. From the echelle equation we find, for constant $\alpha$ and $\gamma$, that the angular dispersion is

$$\frac{d\beta}{d\lambda} = \frac{m}{\sigma\cos\gamma\cos\beta} = \frac{2\sin\theta_B\cos\theta}{\lambda\cos(\theta_B - \theta)} \quad \text{(at blaze peak)} \quad . \tag{2}$$

If we take $\theta = 0$, equation (2) shows clearly that the angular dispersion of a grating depends only on the angle at which it is used. The angular spread of one echelle order $\delta\beta$ is

$$\delta\beta = \frac{\lambda}{\sigma\cos\gamma\cos\beta} = \frac{2\sin\theta_B\cos\theta}{m\cos\beta} \quad , \tag{3}$$

where $\cos\beta$ is taken at the blaze peak. If the echelle is used with camera optics of focal length $f_2$, then at the focal surface the length of one echelle order $\ell = f_2\delta\beta$. The free spectral range $\Delta\lambda$, the wavelength difference between two wavelengths in successive orders at the same angle $\beta$, is

$$\Delta\lambda = \frac{\lambda}{m} = \frac{\lambda^2}{2\sigma\cos\gamma\cos\theta\sin\theta_B} \quad . \tag{4}$$

The plate factor, or reciprocal linear dispersion, is $P = (f_2 d\beta/d\lambda)^{-1}$. If we assume the cross-dispersion element is somewhere in the

collimated spectrograph beam, and that its total angular dispersion is $d\beta'/d\lambda$, then the separation between adjacent echelle orders $\Delta x = f_2 \Delta\lambda(d\beta'/d\lambda)$. Various types and locations of this element are considered below.

As an illustration of echelle properties, consider an echelle with a blaze angle of 63°.5. Figure 2 shows $\lambda d\beta/d\lambda$ for such an echelle as a function of wavelength. For comparison, the same quantity is

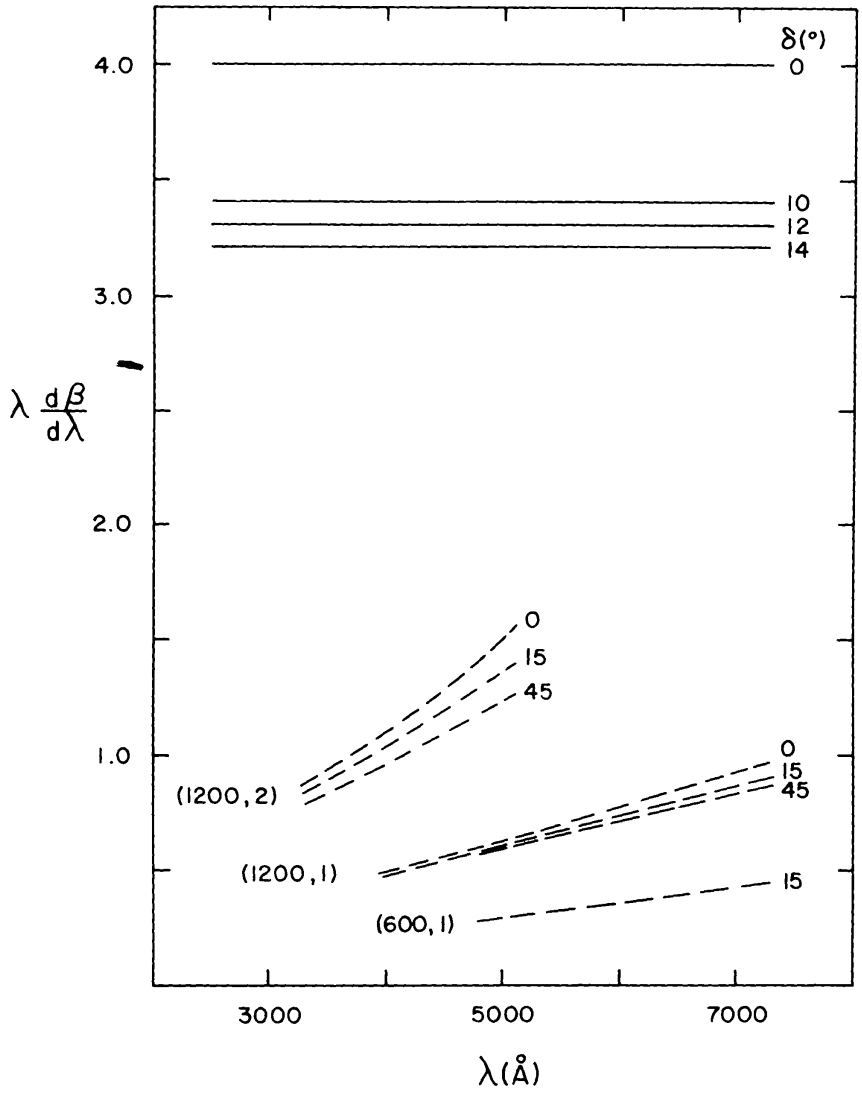


FIG. 2 — Comparison of echelle angular dispersion, $\theta_B = 63°.5$, shown with solid lines, with that of various gratings with small blaze angle, shown with dashed lines. $\delta = \alpha - \beta$ = angle of deviation. The numbers in parentheses are the grooves/mm and order number, in that order.

shown for a 600- or 1200-groove/mm grating used in first or second order. For each element, various angles of deviation $\delta$ between the incident and diffracted beams are assumed, where $\delta = \alpha - \beta = 2\theta$ for the echelle. The results of Figure 2 are derived assuming $\gamma = 0$. The larger angular dispersion of the echelle means, of course, that the plate factor of a grating spectrograph can be obtained with an echelle spectrograph using a camera of shorter focal length. Figure 2 also shows clearly that, for an echelle, $\theta$ should be kept as small as practical so that the high angular dispersion is maintained. As pointed out by Burton and Reay (1970), it is essential to have $\theta > 0$ in order to avoid light loss because of back reflection of the incident light.

The requirement that $\theta$ be small to have high angular dispersion, coupled with the necessity of separating the incident and diffracted beams, means a compromise in the choice of $\theta$. For a spectrograph with an input beam of about $f/8$, an angle $\theta = 6°$ is about the smallest practical value. In the results which follow, this value is assumed. Echelle plate factors for various camera focal lengths, as a function of wavelength, are shown in Figure 3. The results clearly show that plate factors typical of large coudé spectrographs can be obtained with echelle spectrographs having relatively short cameras.

As further illustration of echelle properties, consider two echelles, one with 58 grooves/mm and one with 73 grooves/mm, each with a 63°.5 blaze angle. A choice of groove spacing in this range is suitable for the visible and near ultraviolet because coarser echelles have narrower blaze functions and require greater cross dispersion for adequate order separation, while smaller groove spacing means a larger echelle order length, and hence a larger camera to record an entire order. Figure 4 shows the angular spread of echelle orders, as computed from equation (3) for $\theta = 6°$, for each of the two echelles assumed above. Also shown are lines relating the spread $\delta\beta$ to the echelle order length for several camera focal lengths. Assume, for example, a 58-groove/mm echelle at 6400 Å, which gives $\delta\beta = 0.07$ radian. For a 20-cm camera we find, therefore, an order length of 14 mm. It is clear from Figure 4 that, except for long cameras at the longer wavelengths, entire echelle orders can be recorded by available image tubes. The total spectral coverage in a single exposure depends on the number of orders recorded,

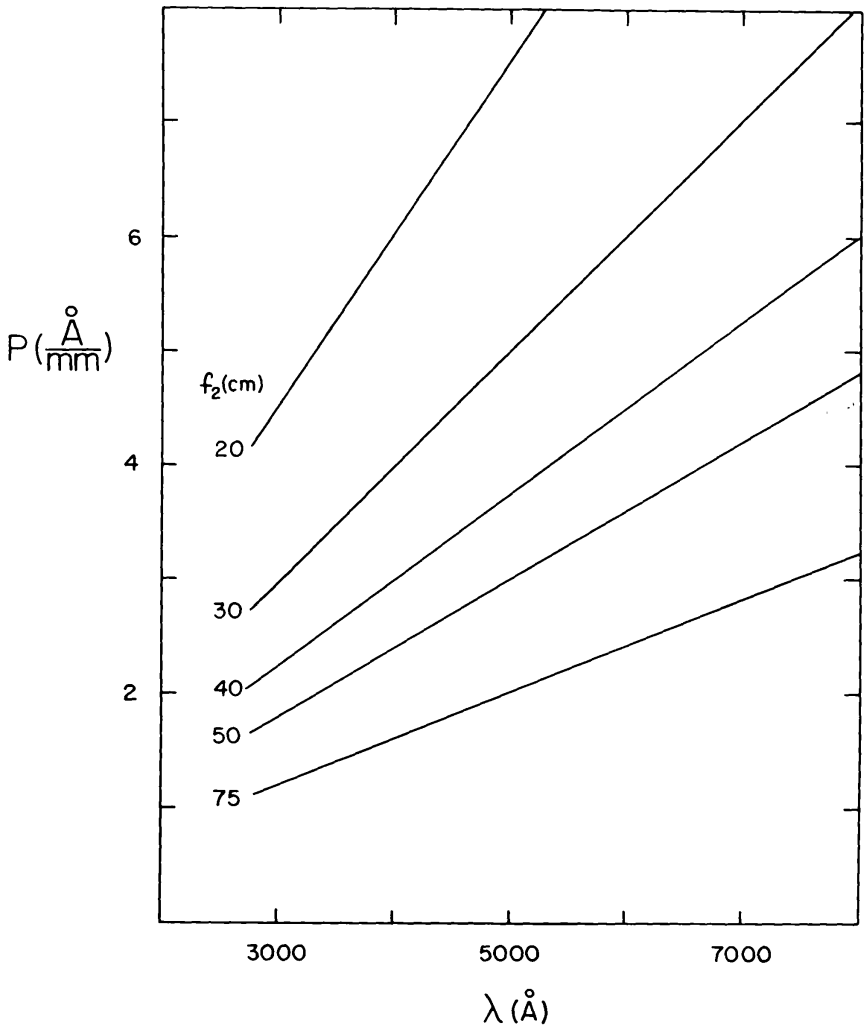


FIG. 3 — Echelle plate factors, or reciprocal linear dispersions, for various camera focal lengths $f_2$. $\theta_B = 63.5$, $\theta = 6°$.

which in turn depends on the amount of cross dispersion and the camera field. Examples are discussed below.

Because $\delta\beta$ is typically a few degrees, any wavelength will appear in some order near the blaze peak. Hence an echelle can be thought of as effectively blazed for all wavelengths. There is, however, an intensity distribution across the blaze peak which determines the true echelle efficiency at a given wavelength. As for any grating, this distribution is determined by the effective width of a single echelle facet. From Figure 1 we see that this width is

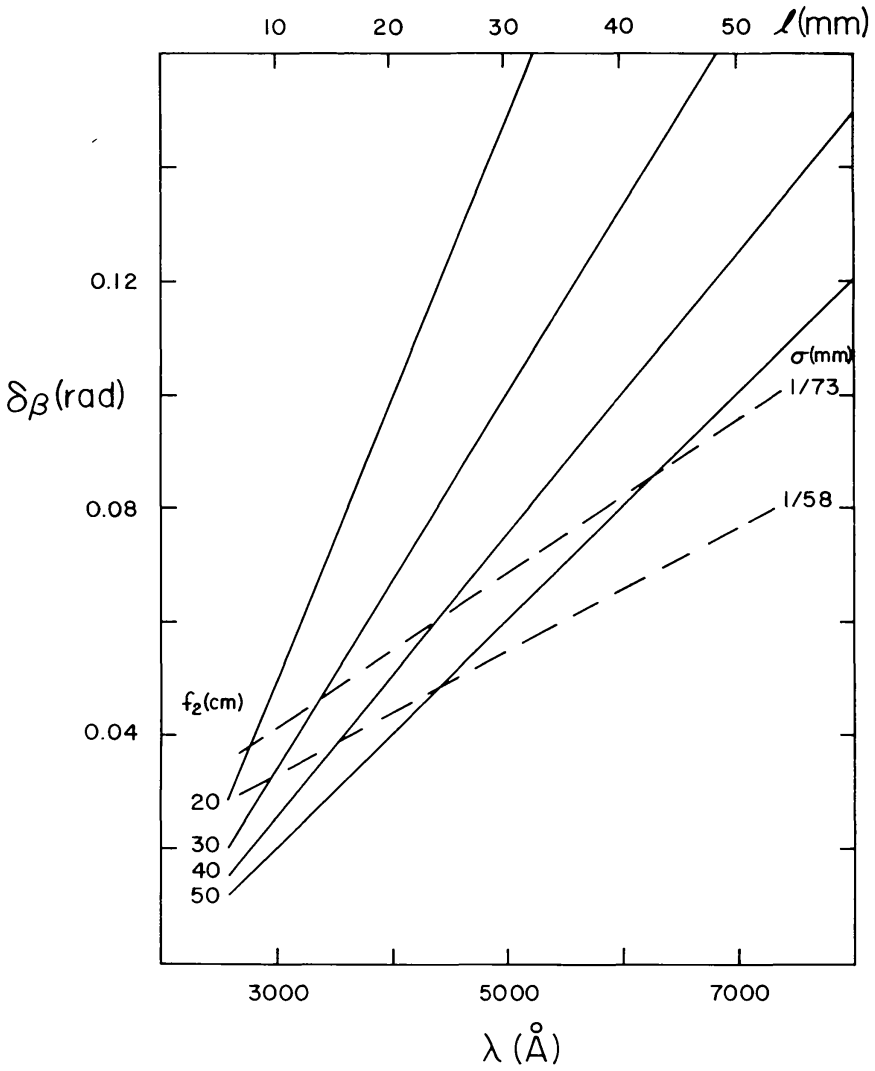


FIG. 4 — Angular spread of single echelle orders and echelle order length for two echelle groove spacings. For both echelles $\theta_B = 63.^\circ 5$, $\theta = 6^\circ$.

less than the total facet width by an amount depending on $\theta$. By simple geometry the effective width $s' = s(1 - \tan\theta \tan\theta_B)$, where the facet width $s = \sigma \cos\theta_B$. For a typical echelle $s >> \lambda$, and the angular separation of the primary minima of the single-slit diffraction pattern is $\delta\phi = 2\lambda/s'$. Using equation (3), with $\gamma = 0$, we find that $\delta\beta/\delta\phi \simeq \cos\alpha/2 \cos\beta = \cos(\theta_B + \theta)/2 \cos(\theta_B - \theta)$. As $\theta$ increases from zero, a single order spans somewhat less of the blaze peak, and the variation of intensity across the order is less pronounced. The portion of the blaze function which is used at

various $\theta$ is shown in Figure 5. In the most favorable case, a monochromatic wavelength is located at the blaze peak, with most of the radiation in a single order. In the least favorable case, most of the radiation is distributed evenly between two orders located symmetrically about the blaze peak. For $\theta = 6°$, these orders are at the 0.69 points of the blaze distribution.

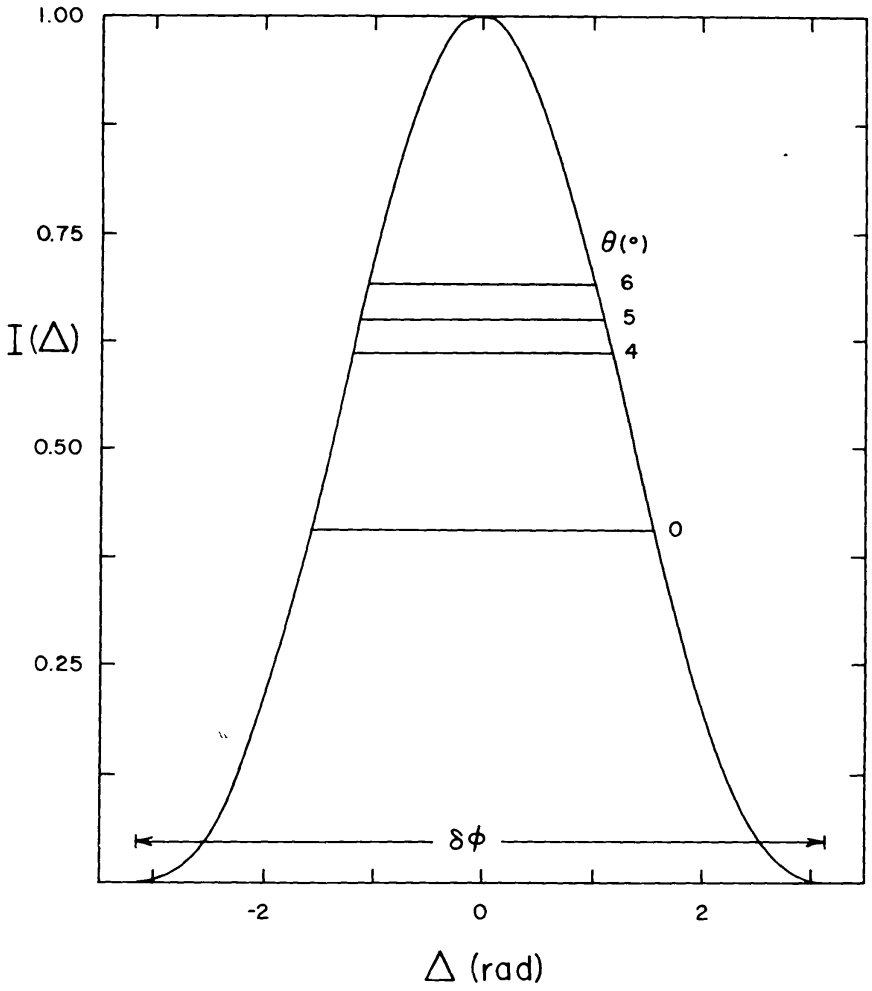


FIG. 5 — Echelle blaze function and portion of it used for various values of $\theta$. $I(\Delta) = (\sin \Delta / \Delta)^2$, where $\Delta = (\pi/\lambda)s' \sin\phi$. See text for definitions of remaining symbols.

Because of the variation in echelle efficiency across each echelle order, a spectrum properly exposed at the blaze peak will be underexposed at the ends of the orders, where the wavelength

separations are equal to the free spectral range. This variation of efficiency at short intervals throughout the spectrum complicates the problem of fixing background intensities in stellar spectra, and careful calibration is necessary. Another problem with echelle spectra is the varying angular dispersion along each order. According to equation (2) the angular dispersion changes by several percent across a single order, thereby requiring the measurement of more comparison lines and careful use of wavelength reduction formulae. These disadvantages are the price paid for the two-dimensional format.

## General Spectrograph Properties

One of the significant advantages of an echelle over a small blaze-angle grating is the larger throughput obtained with the echelle when both elements are used at the same resolving power. The throughput is defined as the monochromatic flux collected by the receiver assuming that the source has a luminance of unity. Let us now determine the nature of this advantage.

Consider the layout shown in Figure 6 consisting of a telescope of diameter $D$ and focal length $f$, a spectrograph with entrance slit

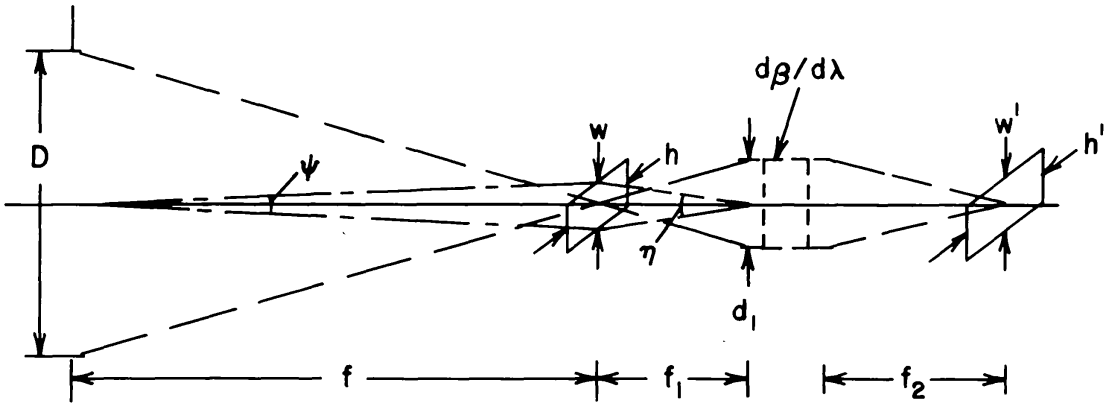


FIG. 6 — General layout of a telescope and spectrograph. See text for definitions of symbols.

width $w$ and slit height $h$, collimator of diameter $d_1$, and collimator and camera focal lengths of $f_1$ and $f_2$, respectively. The angles subtended by the slit on the sky are $\psi = w/f$ and $\psi' = h/f$, respectively; the angles subtended by the slit at the collimator are

$\eta = w/f_1$ and $\eta' = h/f_1$, respectively; the dispersing element has angular dispersion $d\beta/d\lambda$; and the projected slit width and height in the camera focal plane are $w' = w(f_2/f_1)$ and $h' = h(f_2/f_1)$, respectively. The spectral purity $\delta\lambda$ is the wavelength difference between two monochromatic wavelengths whose images are just resolvable for an entrance slit width $w$. A simple calculation gives

$$\delta\lambda = \frac{w}{f_1(d\beta/d\lambda)} = \frac{D\psi}{d_1} \cdot \frac{1}{d\beta/d\lambda} \quad , \tag{5}$$

where $D/f = d_1/f_1$. The attainable spectral resolving power $\mathcal{R} = \lambda/\delta\lambda$, and from equation (5) we find

$$\mathcal{R} = (d_1/D\psi) \cdot \lambda d\beta/d\lambda \quad . \tag{6}$$

It is clear from this expression that the resolving power for a given telescope, with a given angular slit width $\psi$, depends on the collimator size and the angular dispersion of the dispersing element.

As shown by Jacquinot (1954), the throughput of a spectrograph is the product of the collimator area, the solid angle of the entrance slit subtended at the collimator, and the spectrograph transmittance $\tau$. Denoting the throughput by $\mathcal{L}$, we find

$$\mathcal{L} = \tau(\pi d_1^2/4)\eta\eta' = \tau(\pi D^2/4)\psi\psi' \quad . \tag{7}$$

Forming the product $\mathcal{L}\mathcal{R}$, we get

$$\mathcal{L}\mathcal{R} = \tau(\pi d_1/4) \cdot (D\psi')\lambda d\beta/d\lambda \quad . \tag{8}$$

If we assume $D\psi'$ is constant, where $\psi'$ is the seeing disk angular diameter for a stellar source, then we see that, for a given telescope and spectrograph combination, the product $\mathcal{L}\mathcal{R}$ is constant. To increase this product for a given telescope means a larger collimator and/or larger angular dispersion.

We can use equation (8) to compare an echelle instrument with a small blaze-angle grating instrument, used on the same telescope under similar seeing conditions. Assume a stellar source with seeing disk diameter $\psi'$, and $\psi < \psi'$. Denoting the two instruments by subscripts $e$ and $g$, we find

$$\left(\frac{\mathcal{L}_e}{\mathcal{L}_g}\right)_{\mathcal{R}_e=\mathcal{R}_g} = \left(\frac{\mathcal{R}_e}{\mathcal{R}_g}\right)\mathcal{L}_e = \mathcal{L}_g = \frac{d_{1e}(d\beta/d\lambda)_e}{d_{1g}(d\beta/d\lambda)_g} \quad . \tag{9}$$

For a stellar source, with the spectrograph slit such that $\psi \geq \psi'$, all of the light passes the slit and only the second part of equation (9) applies. From Figure 2 for $\lambda$ 4200, we find that the ratios of angular dispersion in equation (9) are about 6 and 3, for a 1200-groove/mm grating used in first and second order, respectively. For the grating, $\delta = 15°$ is used; for the echelle, $\delta = 12°$ is taken. If $d_{1e} = d_{1g}$, then the echelle instrument has a significant advantage in either throughput or resolving power. On the other hand, a grating instrument, with either the throughput or resolving power equal to that of an echelle instrument, must have a larger collimator by the angular dispersion ratios given above. Recent results of Harrison and Thompson (1970) show that high-quality echelles, as large as 210 × 410-mm ruled area and able to accept fully about a 15-cm beam for $\theta = 6°$, can now be ruled. Hence a large echelle instrument will have a real advantage whenever spectral resolution is of prime importance.

The conclusions of the preceding paragraph are true in general, though they are particularly relevant when an echelle instrument is used as a scanning spectrometer with an exit slit and a photomultiplier detector. When considering photographic or image-tube recording of large spectral regions, spectrograph speed is also an important consideration, particularly for faint objects. Consider now the photographic speed of a spectrograph, assuming the entrance slit is narrower than the seeing disk, and with the final spectrum widened to a height $H$. Using the results of Bowen (1952) for this situation (his case II) we find, in our notation,

$$\text{Speed} = \frac{K\tau w' P}{(\mathfrak{F}_2 \psi')^2} \cdot \frac{h'}{H} \quad , \tag{10}$$

where $K$ is a constant, $P$ is the plate factor, and $\mathfrak{F}_2 = d_1/f_2$ is the camera focal ratio. The relative speed of an echelle spectrograph as compared with a grating spectrograph, if one assumes the same telescope and seeing conditions, equal spectrum widening, and equal projected slit widths, is

$$\frac{\text{Speed}\,(e)}{\text{Speed}\,(g)} = \frac{\tau_e P_e h'_e}{\tau_g P_g h'_g} \left( \frac{\mathfrak{F}_{2g}}{\mathfrak{F}_{2e}} \right)^2 \quad . \tag{11}$$

With cameras of the same focal ratio, we have $h'_e = h'_g$, and hence the relative speed depends only on the spectrograph trans-

mittances and plate factors. With cameras giving the same plate factor, we have $h'_e/h'_g = \mathfrak{I}_{2e}/\mathfrak{I}_{2g}$, and therefore speed $(e)$/speed $(g) = (\tau_e/\tau_g)(\mathfrak{I}_{2g}/\mathfrak{I}_{2e})$.

The advantages of an echelle for high resolution are most easily appreciated by examining the results in Figure 7. Shown are plate factors at λ 4200, as a function of camera focal length, for

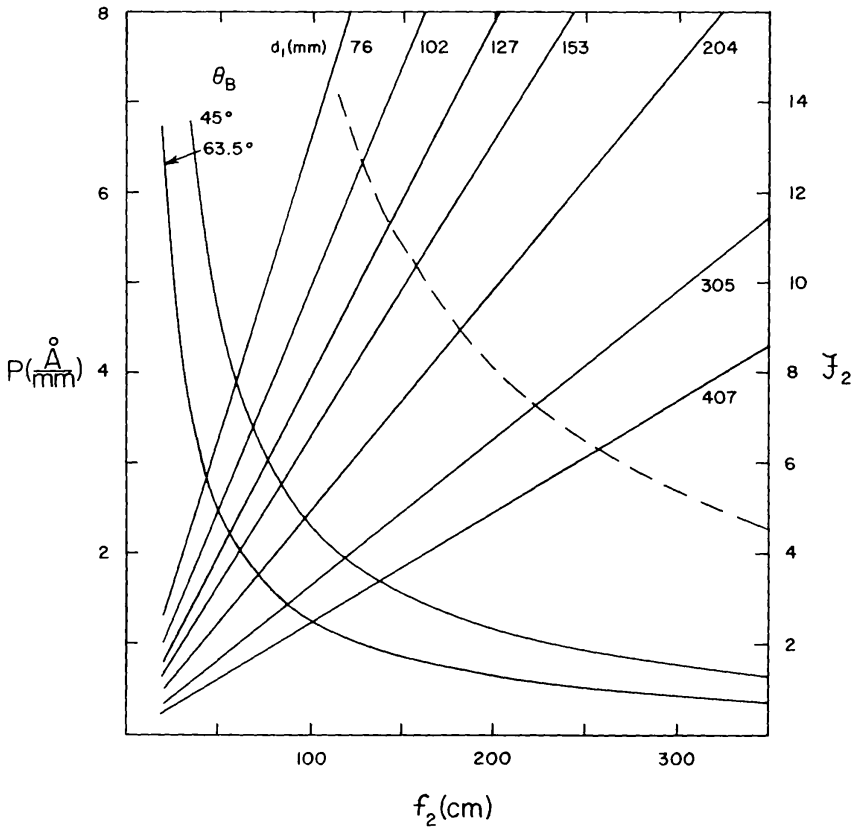


FIG. 7 — Plate factors for two echelles (solid lines) and one grating (dashed line) as a function of camera focal length, for λ 4200. Camera focal ratios for various collimator beam diameters. For the echelles $\delta = 12°$; for the grating $\delta = 15°$.

echelles with blaze angles of 45°, 63°.5, and for a 600-groove/mm grating used in second order. Also shown in Figure 7 are straight lines relating the camera focal length and focal ratio for various collimator diameters. Suppose, for example, that a plate factor of 5 Å/mm is desired. For the echelle with $\theta_B = 63°.5$, a camera with $f_2 = 25$ cm is required, while for the grating $f_2 \simeq 160$ cm is needed.

Assuming an echelle collimator diameter of 102 mm, fully accepted by an echelle 300 mm wide with $\theta = 6°$, we find that an $f/2.4$ camera is needed. For the grating, on the other hand, a beam diameter of 305 mm gives an $f/5.3$ camera. If the instrument transmittances are comparable, $\tau_e \sim \tau_g$, then the echelle spectrograph clearly has an advantage in speed at this dispersion. We also see from this example that, for equal plate factors, an echelle instrument is relatively much smaller than a grating instrument. These same conclusions, with regard to speed and size, hold for still higher dispersions. The assumption that $\tau_e \sim \tau_g$ is reasonable, if we compare a Cassegrain echelle spectrograph with a coudé grating spectrograph. The extra mirrors required to get the light to the coudé focus will have about as much light loss as the cross-dispersion element of an echelle instrument. If, however, we compare an echelle spectrograph with a conventional grating instrument used at the same telescope focus, then $\tau_e < \tau_g$ because of the extra dispersing element in the former instrument.

The spectral resolving power which is obtained for a given projected slit width is easily calculated from equation (6). Substituting for the angular entrance slit width $\psi$ in terms of the projected slit width $w'$, we find $\mathcal{R} = (d_1 \Im_2 / w')\lambda d\beta/d\lambda$. Figure 8 shows the resolving power for $w' = 15\,\mu$, for various collimator beam diameters, at $\lambda$ 4200. The solid lines are for an echelle with $\theta_B = 63°.5$; the dashed lines are for a 600-groove/mm grating used in second order.

## Echelle Spectrograph Design Considerations

In considering various spectrograph designs, the prime consideration is to have instrument performance limited only by seeing or detector resolution, and not by geometrical aberrations. Abberations are negligible and seeing-limited performance is achieved with an echelle instrument used at a coudé focus at about $f/30$ (Liller 1970). For faster instruments, such as the $f/13.6$ Cassegrain echelle spectrograph at the University of Wisconsin (Schroeder and Anderson 1970), careful attention is given to the reduction of aberrations. This particular design, a modified Czerny-Turner arrangement, is limited to about $f/10$ or slower, and faster input beams require a different arrangement.

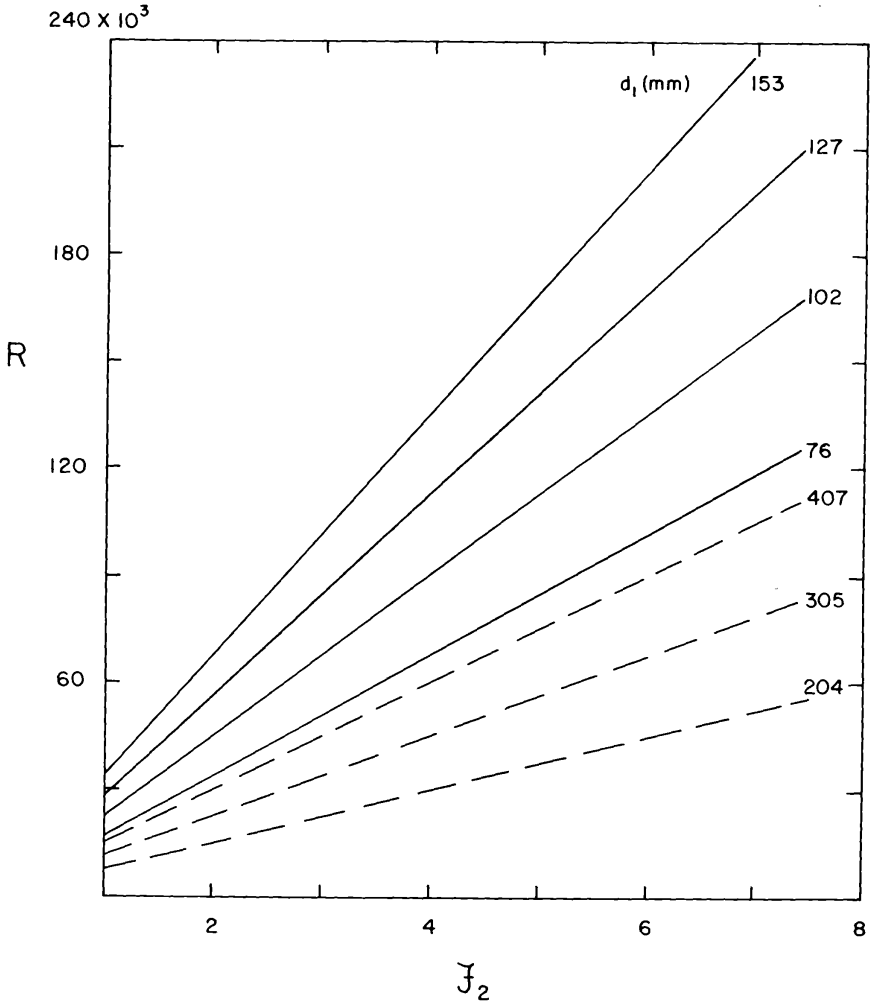


FIG. 8 — Spectral resolving power at λ 4200 for a projected slit width of 15 μ. Solid lines denote an echelle, $\theta_B = 63°.5$, $\theta = 6°$, for several beam diameters. Dashed lines denote a grating, 600 grooves/mm, second order, for several beam diameters.

A reasonable Cassegrain design for an *f*/7.8 beam is based on a choice of collimator and camera each of which is essentially aberration free, at least for a stellar object on axis. For the collimator, the choice is between a paraboloid used on axis with a flat mirror to fold the telescope beam, and an off-axis paraboloid. The choice of the first option is preferable for two reasons: (1) For a source displaced from the telescope axis, the aberrations of an on-axis paraboloid are smaller; and (2) For a folded system, the long dimension of the spectrograph is parallel to the back of the

mirror cell, and rigid mounting of the instrument is more easily achieved. Because of the secondary shadow of the telescope, the folding flat does not vignette the collimator beam.

The general layout of an echelle spectrograph, from the Cassegrain focus through the cross-dispersion element, is shown in Figure 9. After looking at various ways of getting the necessary cross dispersion, a reflection grating located in the dispersed beam

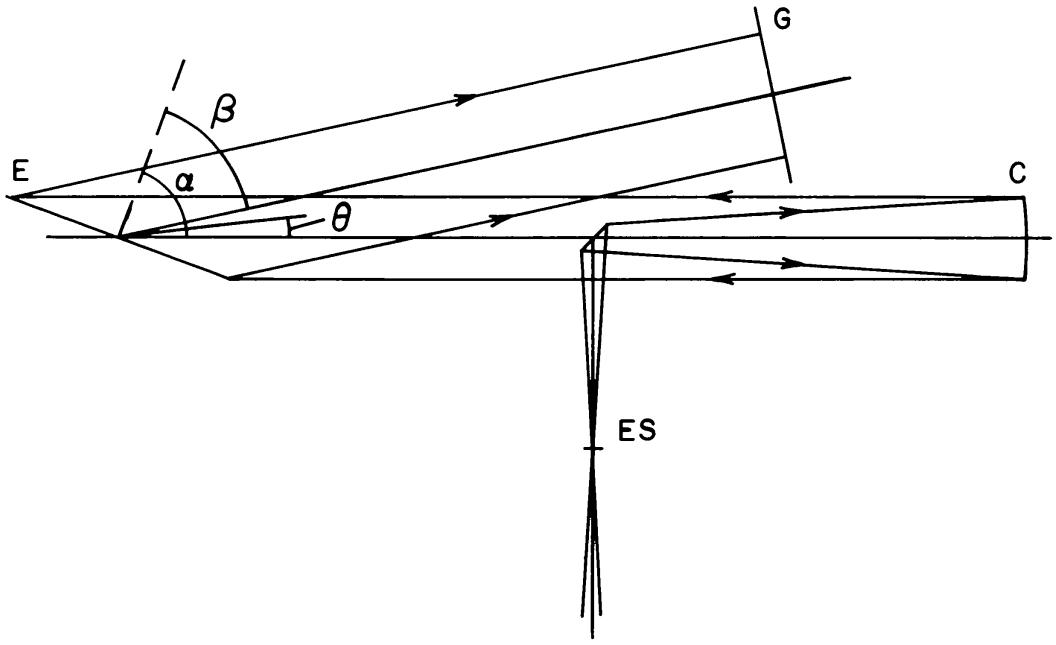


FIG. 9 — Cassegrain echelle spectrograph layout, through the cross-dispersion element. Parabolic collimator $C$, echelle $E$ with $\theta_B = 63.^\circ 5$, $\theta = 6^\circ$; reflection grating $G$ for cross dispersion; entrance slit $ES$.

of the echelle was chosen. Other options are a prism or transmission grating located in front of the echelle and used double pass, a prism located in the dispersed beam and used either single or double pass, or a single-pass transmission grating in the dispersed beam. These options were rejected for the following reasons.

Quartz or glass prisms, though more efficient than gratings, do not separate the echelle orders sufficiently, except for long-focus cameras. A 30° quartz prism, for example, used double pass with a camera of 70-cm focal length and a 73-groove/mm echelle, gives

order separations of about 0.7 mm and 0.5 mm at λ 4200 and λ 6200, respectively. These separations are not enough for widened stellar spectra and accompanying comparison spectra, and the situation is worse for shorter cameras. A grating, on the other hand, has the advantage that the amount of dispersion is easily changed to suit a particular situation simply by changing gratings, or by using a different grating order.

A transmission grating at the echelle has two defects. Because it is used double pass, the overall efficiency is markedly less than that of a single-pass grating, particularly at wavelengths off the peak of the blaze. The other problem with this arrangement is the spectral line tilt introduced because the light is partly dispersed before striking the echelle. This partial dispersion means that $\gamma$ in equation (1) is not equal to zero, except at one wavelength. For a given wavelength, we can determine how a change in $\gamma$, at constant $\alpha$, affects $\beta$. From equations (1) and (2), we find $d\beta/d\gamma = \tan\gamma \cdot \lambda d\beta/d\lambda$, where $d\beta/d\gamma$ is the tangent of the angle between a line parallel to the echelle rulings and a line along the focused spectral image. Because $\gamma$ is a function of wavelength, we see that the orientation of spectral lines depends upon their location on the focal surface. Over a reasonable camera field the orientation will vary by several degrees. If, however, all the cross dispersion is done on the diffracted beam from the echelle, then $\gamma = 0$ for all wavelengths and varying line tilt is absent.

A transmission grating in the dispersed beam has one major problem: The wavelength at the center of the camera field can be changed only by rotating the entire camera about an axis on the grating face. It is preferable to have a rigidly mounted camera, and use a rotatable reflection grating to select the desired wavelength range. Any grating in the dispersed beam must, of course, be large enough to accept all of this beam without vignetting, which means a grating roughly twice as long as it is wide.

The logical choice of spectrograph cameras is from the family of Schmidt or Schmidt-Cassegrain cameras, though a design suited for one type of detector may not be satisfactory for another. For direct photographic recording, a conventional Schmidt camera, with corrector and field flattener, provides good spectral coverage with little vignetting. For image-tube spectroscopy, however, some type of folded Schmidt camera is necessary to avoid the large amount of

vignetting which would otherwise occur. One possible camera arrangement is shown in Figure 10; C I is a folded Schmidt for

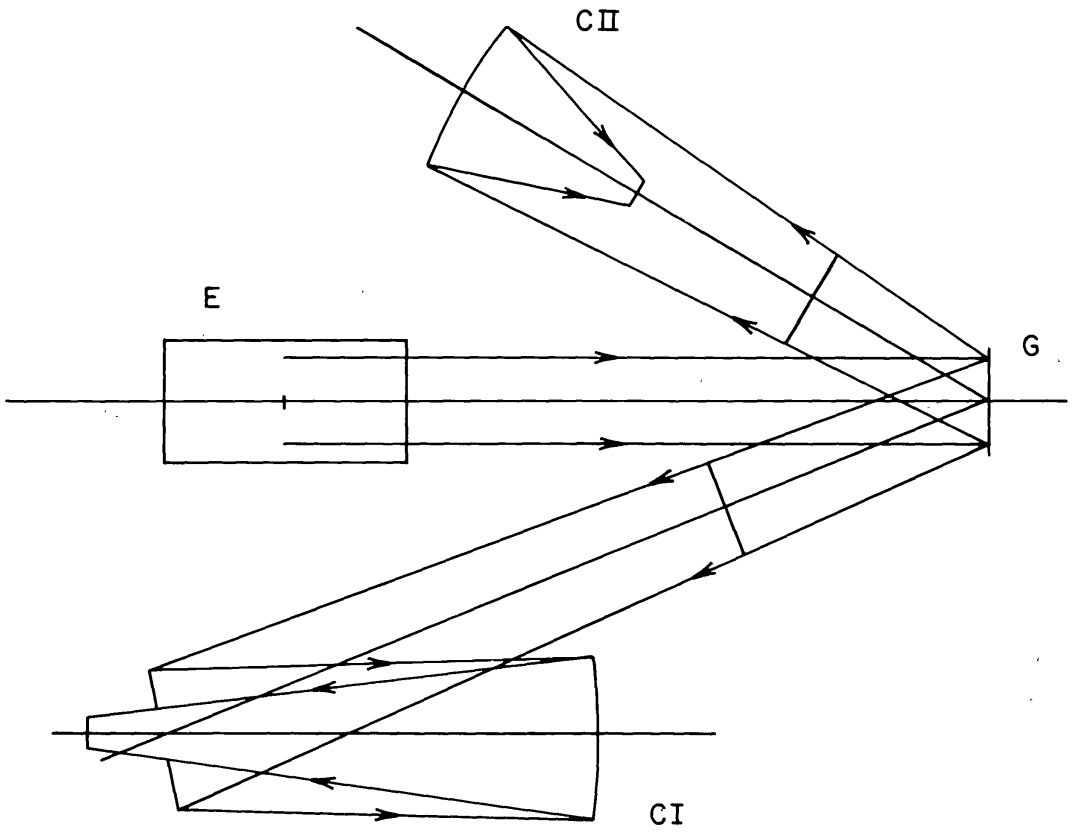


FIG. 10 — Echelle spectrograph camera layout. Typical photographic Schmidt camera (C II) and folded image-tube Schmidt camera (C I) are shown. The plane of Figure 10 is perpendicular to that of Figure 9, and contains the line joining the centers of the echelle and grating.

image tubes, and C II is a photographic Schmidt. In this configuration, both cameras are permanently mounted, and the switch from one to the other is done by turning over the grating to get the proper blaze direction. For any folded camera, be it the type shown or a Schmidt-Cassegrain type, careful attention must be given to vignetting. C I, for example, has an average of about 25 percent vignetting over a 4° circular field. The cameras shown in Figure 10 are representative and, because of the variety of possible choices, no further discussion of details is given here.

Let us now consider such features as beam size for various echelle dimensions, order separation, spectral coverage, and format at the focal surface. An echelle of 58 grooves/mm, blaze angle 63°.5, with $\theta = 6°$, is assumed in the remaining discussion. Let $W$ denote the long dimension of the echelle, hereafter called the width. The width of the echelle is filled when the collimator beam diameter $d_1 = W \cos \alpha = W \cos(\theta_B + \theta)$. With the above values, we get $d_1 = 0.35W$; thus a 102-mm beam requires a minimum echelle width of 292 mm. The height of the diffracted beam, in the direction of the echelle dispersion, $d_2 = W \cos\beta = d_1 \cos\beta/\cos\alpha$. For the given angles $d_2 \simeq 1.53 d_1$ at the echelle blaze peak. Because of the beam expansion in one direction, the diffracted beam is elliptical in cross section, and the grating and camera must be large enough to accept this beam over the desired field.

The order separation $\Delta x$ given by the grating is

$$\Delta x = f_2 \, \Delta\lambda (d\beta'/d\lambda) = f_2 \, \Delta\lambda \cdot m'/\sigma \cos\beta' \quad , \tag{12}$$

where $\Delta\lambda$ is the free spectral range given by equation (4), and the primed quantities refer to the grating parameters. Because of the $\lambda^2$ dependence of $\Delta x$, the order separation increases rapidly from blue to red. It is possible, however, to keep $\Delta x$ within a factor of two from 3500 Å to 7000 Å by using the grating in first order for $\lambda > 5000$, and in second order for $\lambda < 5000$. A first-order grating blaze of about 7500 Å gives the best overall efficiency over the near ultraviolet and visible. Figure 11 shows the free spectral range and order separation, adjusted to 1.0 mm at 5000 Å in first order and with $\beta' \sim 0$, for the echelle chosen. With a minimum separation of 1 mm, a stellar spectrum widened to 0.6 mm–0.7 mm and short comparison spectra on either side can be photographed without overlap.

The spectral coverage $\lambda^* = \Delta\beta' (d\lambda/d\beta')$, where $\Delta\beta'$ is the angular size of the camera field in the direction of the grating dispersion. Substituting for the grating angular dispersion from equation (12), we get $\lambda^* = \Delta\beta' \cdot \sigma' \cos\beta'/m' = f_2 \, \Delta\beta' (\Delta\lambda/\Delta x)$. If we choose $\Delta x = 1.0$ mm at $\lambda$ 5000 for all cameras, then $\Delta\lambda/\Delta x$ is a constant, and the spectral coverage is directly proportional to the camera focal length and field angle. For $\Delta\beta' = 4°$ we get the results shown in Figure 12 for $m' = 1, 2$. With an unfolded photographic Schmidt camera $\Delta\beta' = 8°$ can be used without serious vignetting by the

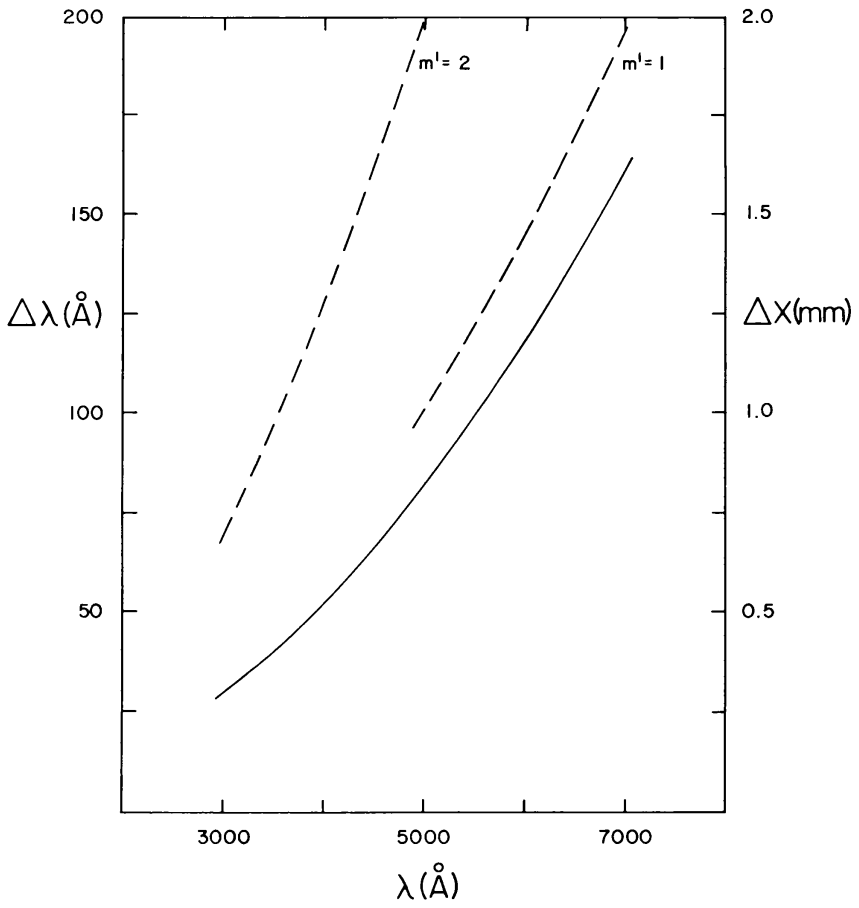


FIG. 11 — Free spectral range $\Delta\lambda$ (solid line) and order separation $\Delta x$ (dashed lines) for a 58-groove/mm echelle, $\theta_B = 63.^\circ 5$, $\theta = 6^\circ$. The order separation is set at 1.0 mm at $\lambda$ 5000 in the first order of the cross-dispersion grating. Results shown in Figures 12 and 13 are for an echelle with the above parameters.

plate, and the spectral coverage is double that shown in Figure 12. Also shown in Figure 12 is spectral coverage for other minimum order separations.

Choice of the grating giving the required minimum order separation for a given camera can be determined from Figure 13. Shown there are the order separations at 5000 Å ($m' = 1$) and 3500 Å ($m' = 2$) for various grating constants as a function of camera focal length. For $f_2 = 20$ cm, for example, a grating with 600 grooves/mm gives the necessary cross dispersion. The results shown in Figures 12 and 13 are for $\beta' = 0$. For nonzero $\beta'$ the equations given above should be used.

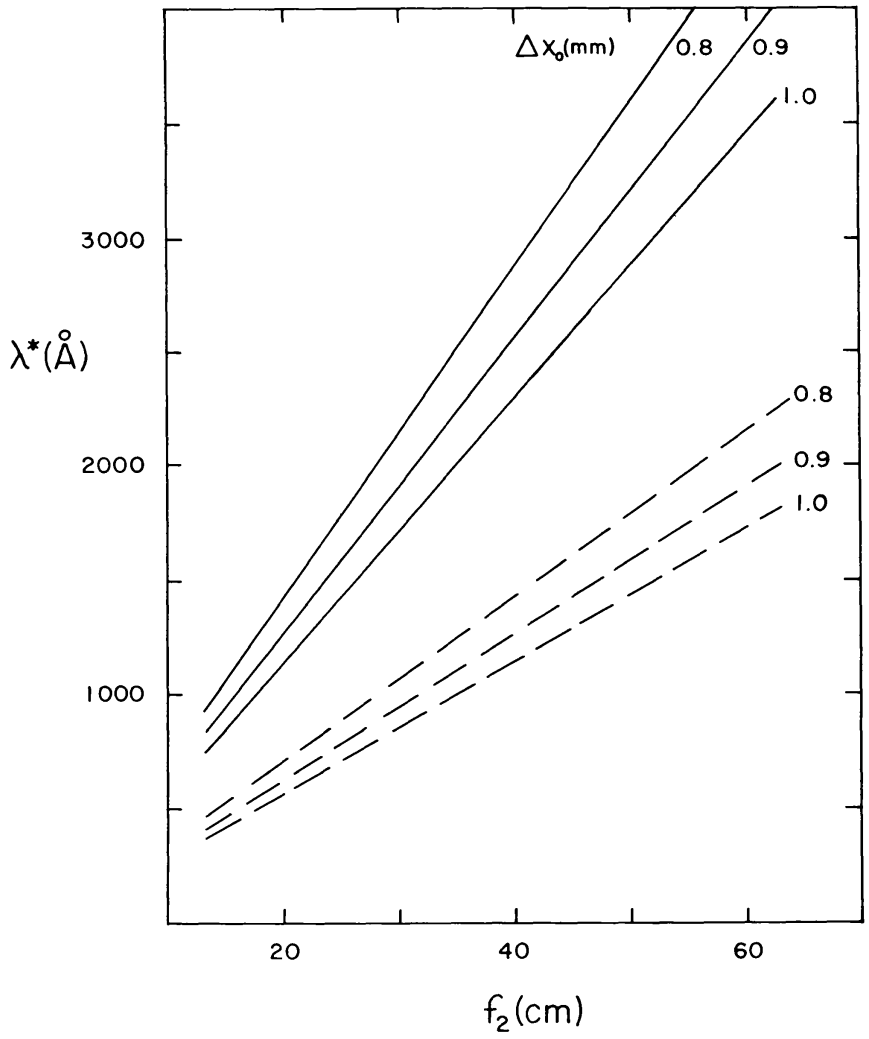


FIG. 12 — Spectral coverage $\lambda^*$ for a total camera field width of 4°. $\Delta x_0$ = order separation at $\lambda$ 5000 in first order (solid lines) and $\lambda$ 3500 in second order (dashed lines). The grating angle of diffraction $\beta'$ is assumed to be small. Camera focal length is $f_2$.

The format at the camera focal surface is the well-known stacked spectrum; examples of stellar spectra in such formats are shown by Liller (1970) and Schroeder and Anderson (1970). Assuming $\Delta\beta$ is the angular size of the camera field in the direction of the echelle dispersion, we see from equation (3) that an entire echelle order is recorded as long as $\delta\beta < \Delta\beta$. For the echelle selected, and with $\Delta\beta = 4°$, we see from Figure 4 that no wavelengths are missed shortward of 6400 Å. In this case about nine percent of an echelle

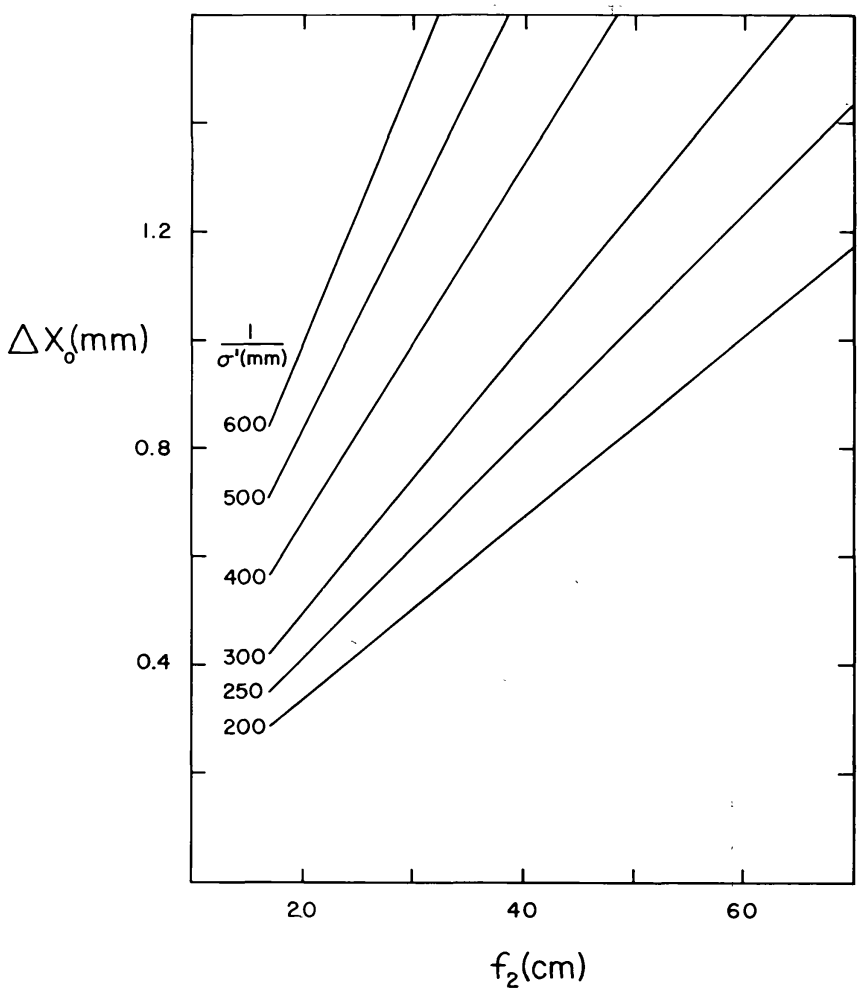


FIG. 13 — Minimum order separation for various grating constants $\sigma'$. See caption of Figure 12 for definitions of symbols.

order near 7000 Å is missed. Because $\delta\beta$ depends on the echelle groove spacing, the coverage of complete orders for echelles with more grooves/mm requires larger $\Delta\beta$. An instrument with the parameters given above has good spectral coverage with moderate camera fields.

It is obvious that each optical element within a spectrograph should be as efficient as possible. An echelle spectrograph with two dispersing elements will have lower transmittance, for example, than a conventional Cassegrain grating spectrograph. However, an echelle instrument does not compete with such a grating spectro-

graph, but rather it complements it. The former is for high dispersion; the latter is for low and medium dispersion. Transmittance comparisons should be restricted to echelle spectrographs (Cassegrain or coudé) versus coudé grating spectrographs. With echelle efficiencies of 70 percent or more (Harrison and Thompson 1970), the overall transmittance of a Cassegrain echelle spectrograph should be comparable to that of a coudé grating instrument.

The writer wishes to thank Dr. Helmut Abt of Kitt Peak National Observatory and Dr. Pat Osmer of Cerro Tololo Inter-American Observatory for many fruitful discussions, and Dr. Arthur Hoag of Kitt Peak National Observatory for making possible an extended stay in Tucson.

## REFERENCES

Bowen, I. S., 1952, *Ap. J.* **116**, 1.
Burton, W. M., and Reay, N. K., 1970, *Applied Optics* **9**, 1227.
Harrison, G. R., 1949, *J. Opt. Soc. Am.* **39**, 522.
Harrison, G. R., and Thompson, S. W., 1970, *J. Opt. Soc. Am.* **60**, 591.
Jacquinot, P., 1954, *J. Opt. Soc. Am.* **44**, 761.
Kopylov, I. M., and Steshenko, N. V., 1965, *Proc. Crimean Astrophys. Obs.* **33**, 308.
Liller, W., 1970, *Applied Optics* **9**, 2332.
Schroeder, D. J., 1967, *Applied Optics* **6**, 1976.
Schroeder, D. J., and Anderson, C. M., 1970, submitted for publication in the *A.J.*